RSC Advances

ROYAL SOCIETY OF CHEMISTRY

www.rsc.org/advances

Fabrication and characterization of PCL/$CaCO_3$ electrospun composite membrane for bone repair

Zhinan Cao[a,b], Dandan Wang[a,b], Lingwei Lv[a,b], Yihong Gong[a,b,*], Yan Li[a,b,*]

[a]Department of Biomedical Engineering, School of Engineering, Sun Yat-sen University, Guangzhou, Guangdong, P.R. China

[b]Guangdong Provincial Key Laboratory of Sensor Technology and Biomedical Instrument, Sun Yat-sen University, Guangzhou, Guangdong, P.R. China

*Corresponding author: Yihong Gong, Telephone: +86-20-39332146; Fax: +86-20-39332146; Email: gongyih@mail.sysu.edu.cn

Yan Li, Telephone: +86-20-39387890; Fax: +86-20-39387890; Email: liyan99@mail.sysu.edu.cn

Abstract

Tissue engineering offers a promising approach to repair bone defects, of which scaffold is an indispensible component. An ideal scaffold should mimic the organic and inorganic compositions of bone. Here, $CaCO_3$/casein microspheres were encapsulated in PCL composite membranes using co-solvent electrospinning to mimic the hierarchical structure and composition of bone ECM. As PCL lacks functional groups to support cell adhesion, gelatin was grafted onto membranes. To find the optimum composition, $CaCO_3$/casein microspheres were entrapped at five different concentrations. Various analytical techniques, including FTIR spectroscopy, XRD, SEM and EDS were applied to characterize the particles and membranes. The $CaCO_3$/casein microparticles were spherical of 1 μm, mainly in vaterite form. The amount of casein was 23.9 ± 1% determined by BCA assay and its presence stabilized $CaCO_3$ in vaterite. After surface modification, the hydrophilicity of membrane was improved while the membrane morphology was not significantly changed; on the membranes, both gelatin and $CaCO_3$/casein vaterite microparticles were evenly distributed. Due to the presence of vaterite, the biomineralization property of composite membrane was significantly enhanced. Furthermore, we compared HMSC proliferation on composite membranes with FDA staining and MTT assay. After cells cultured in osteogenic medium, differentiation potential was investigated by analyzing gene expressions of RUNX2, COL-I and ALP, and monitoring ALP activity. It was found that the presence of $CaCO_3$/casein particles enhanced cell proliferation and differentiation, especially sample P-20 which demonstrated better potential to be used in bone tissue engineering than others.

Key words: vaterite, electrospinning, composite membrane, stem cell, differentiation

1. Introduction

Bone is a dynamic tissue with unique mechanical and biological properties[23]. It mainly consists of organic collagen type I fibers and inorganic hydroxyapatite (HAp) crystals in well organized nanostructure[16]. It may be impaired and inactivated by diseases or accidents. Thus, bone graft is widely needed to replace insufficient bone so as to repair bone defects[11,28,41]. Millions of bone transplantations are performed annually in the world[2,18], making a great clinical need for bone grafts[2]. Limited by a shortage of tissue donor, tissue engineering is a promising approach which is promptly developed with combinations of scaffolds, cells and bioactive agents to reproductive and repair damaged tissue[20,30,45,47].

In order to develop an effective strategy for bone regeneration, the scaffolds should mimic the hierarchical structure and biological functions of natural extracellular matrices (ECM) of bone, which is of organic/inorganic composition. Among various scaffolds[3,4,37,42,44], electrospinning fibrous membranes offer great advantages such as mimicking the nature ECM, fabricated with a simple method and porous[31]. There is a wide range of polymers such as poly(lactic acid) (PLA)[29,30,46], poly(lactic-co-glycolic acid) (PLGA)[33], and poly(ε-caprolactone) (PCL)[32] which can be fabricated as fibrous membranes. More specifically, PCL has advantages of biocompatibility, processability and degradability[6,32]. However, it lacks bioactivity such as osteoconductivity.

Recent researches have been focused on the incorporation of inorganic particles within the polymeric matrix to prepare a superior materials as bone substitutes[6]. There are various inorganic fillers, such as HAp[16], bioactive glass[1], $CaCO_3$[34] and TiO_2[14]. Among them, $CaCO_3$, with the advantage of biocompatibility and simple synthesizing method, has been used in muti-purpose applications[36,38,39]. $CaCO_3$ has three anhydrous crystalline forms: calcite, aragonite and vaterite. Calcite is the most thermodynamically stable form. However for applications such as bone cavity filling biomaterials, the ideal form is vaterite which is of its special structure and unique character, such as high dispersion, high specific surface area. The vaterite form is not thermodynamically stable and easy to transform into rhombohedral calcite[21], thus organic additives are needed to stabilize the vaterite form. Various polymers have been applied to affect the crystallization of $CaCO_3$, such as acrylic acid polymers[19] and poly(sodium 4-styrenesulfonate)[40]. However, none of these additives have

potential to demonstrate osteoconductivity or to improve the bioactivity of $CaCO_3$.

Casein, the most abundant milk protein, demonstrated the potential to enhance biomineralization. It is proline-rich phosphoprotein, possessing four forms, αS_1-, αS_2-, β-, and κ-casein[17]. They are all in amphiphilic structures[8], which have preserved the ability to interact with a wide range of active compounds via functional groups on their primary polypeptide structure, offering a variety of possibilities for reversible binding with active molecules such as Ca and also enhancing Ca absorption[9,43]. Thus β-casein was used to stabilize the crystallization of $CaCO_3$ so as to fabricate vaterite here.

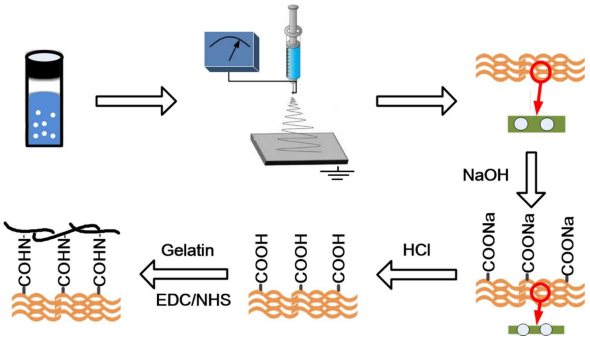

Scheme 1. Preparation of fibrous composite membranes.

In this study, to mimic the hierarchical structure and biological functions of ECM, $CaCO_3$/casein microspheres were encapsulated in PCL using co-solvent-based electrospinning method[26] to fabricate composite fibrous membranes with osteoconductivity (Scheme 1). PCL is a synthetic biomaterial with hydrophobic surface, and lacks functional groups, which is difficult to support cell adhesion[25]. Thus we used gelatin for surface modification[10,22]. To find the optimum composition of membrane, $CaCO_3$/casein microspheres were entrapped at five different concentrations. Several analytical techniques, including Fourier transform infrared (FTIR) spectroscopy, X-ray diffraction (XRD), scanning electron microscopy (SEM) and energy dispersive spectroscopy (EDS) were applied to characterize the particles and membranes. Furthermore, we compared the cell proliferation and differentiation potential on various composite membranes with Fluorescein diacetate (FDA) staining, 3-(4,5-dimethyl-2-thiazolyl)-2,5-diphenyl-2-H-tetrazolium bromide (MTT) assay, gene expression analysis of transcription factors Runt-related transcription factor 2

(RUNX2), collagen type I (COL-I) and alkaline phosphatase (ALP), and ALP activity test.

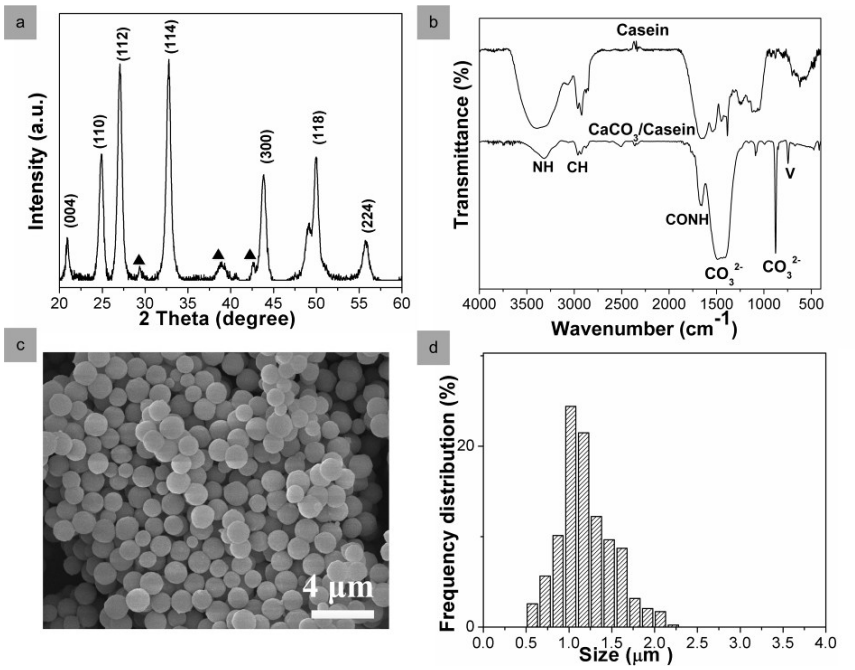

Fig. 1. Characterizations of $CaCO_3$/casein particles. (a) XRD pattern, where ▲ represents peaks belonging to calcite phase; (b) FTIR spectra, where v indicates the characteristic band of vaterite; (c) SEM image; (d) Size distribution.

2. Results and discussion

2.1 Characterization of microparticles and composite membranes

In this study, $CaCO_3$/casein hybrid microparticles were fabricated using co-precipitated method[43]. Several analytical techniques were employed to characterize the microparticles. As shown in Fig. 1a, there are seven main XRD diffraction peaks assigning to (004), (110), (112), (114), (300), (118) and (224) planes of vaterite (JCPDS card No. S # 74-1867). Additionally, three small diffraction peaks of calcite (JCPDS Card No. 86-0174) were observed. All peaks are very broad, indicating $CaCO_3$/casein microparticles were aggregates of nanoparticles. The functional groups in samples were investigated using FTIR (Fig. 1b). The characteristic vaterite band at 751 cm^{-1}[12] was present and the CO_3^{2-} bands were fount at 870 cm^{-1} and 1640 cm^{-1} [24,35]. In addition, due to the presence of casein, -CONH- absorption band at 1650 cm^{-1}, -NH- band at 1541 cm^{-1} and C-H band at 3400 cm^{-1} were all present in the spectrum[43] . However, even calcite diffraction peaks were shown in XRD pattern, there was no

absorption band at 1800 cm^{-1}, which belongs to calcite crystal[13]. The morphology of $CaCO_3$/casein microparticles was characterized by SEM (Fig. 1c). The size was measured using Image J software and its distribution was shown in Fig. 1d. All microparticles were in spherical shape of 1 μm, where its distribution was very narrow. Even though calcite diffraction peaks were present in XRD pattern, the calcite particles which were usually rhombohedral were not observed.

The amount of casein in the as-prepared particles was quantified using a BCA protein assay kit, where it was determined to be 23.9 ± 1% with the encapsulation efficiency of 38.76 ± 1.6%. We speculated that the presence of casein influenced particle formation and also stabilized particles in vaterite form. Organic additives have been proved to be absorbed onto ionic crystals and preceded over all other crystal nucleus surfaces, thus effectively precluded the crystal growth[9]. Here casein was supposed to have two functions, on the one hand, binding to the growth sites of the crystals in order to inhibit crystal growth, on the other hand acting as a heterogeneous nucleator to control and stabilize the precipitating polymorph[5].

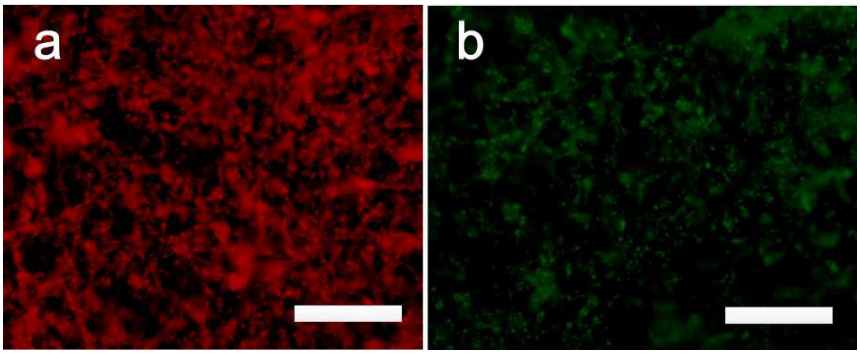

Fig. 2. Distribution of (a) gelatin and (b) casein in membranes after surface modification. Gelatin and casein were labeled with Rhodamine B and FITC respectively. Fluorescence microscope images of P-50 were taken after surface modification. The scale bar is 100 μm.

$CaCO_3$/casein microparticles were entrapped inside PCL fibers through electrospinning to form composite membrane. Since PCL was hydrophobic and lacked functional groups for cell adhesion, the membranes were first treated with NaOH solution to partially hydrolyze PCL and then gelatin was grafted. When looking at P-50 for an example, the water contact angle of as-electrospun membrane was determined to be 113.9 ± 3.7°, while after NaOH treatment, the value decreased

to 76.3 ± 1.3°. Even though the presence of NaOH partially degraded PCL, based on SEM observation, the membrane morphology was not significantly changed with similar fiber diameter; while the entrapped $CaCO_3$/casein microparticles were exposed (Supporting information, Fig. S1). After the surface modification process as described in section 4.2.3, the water contact angle was 66.4 ± 6.0°.

To observe the distribution of gelatin and casein on membranes, we used Rhodamine B labeled gelatin and fluorescein isothiocyanate (FITC) labeled casein for surface modification. Casein has strong affinity with Ca. Thus rely on the casein, we can also tell the distribution of $CaCO_3$/casein microparticles in membrane. As shown in Fig. 2, both gelatin and these microparticles were evenly distributed while lots of $CaCO_3$/casein were present on the surface since some green fluorescence dots were observed.

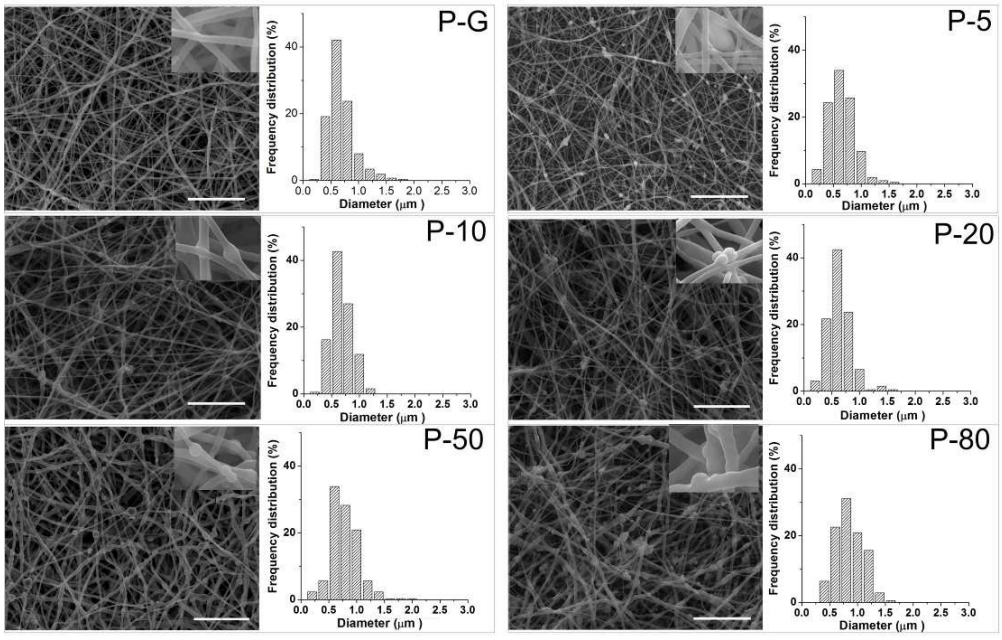

Fig. 3. SEM images and diameter distribution of different composite fibrous membranes after surface modification process completed. The insets are SEM images of fibers at higher magnification. The scale bar is 40 μm.

The morphology of composite membranes was examined using SEM. As shown in Fig. 3, there were no beads in the fiber (insets of each sample) and $CaCO_3$/casein microspheres were evenly distributed across the membranes. The fiber diameters of

different samples were quantified with Image J software, where the diameters were mainly ranging from 400 nm to 1000 nm. While for sample P-80, due to the very high amount of $CaCO_3$/casein, the fiber diameter was slightly larger, ranging from 400 nm to 1200 nm. The average fiber diameters were 476 ± 176 nm, 518 ± 250 nm, 537 ± 211 nm, 646 ± 151 nm, 687 ± 261 nm and 753 ± 245 nm for P-G, P-5, P-10, P-20, P-50 and P-80, respectively. With increase of $CaCO_3$/casein amount, the fiber diameter showed an increasing trend while the difference was not significant.

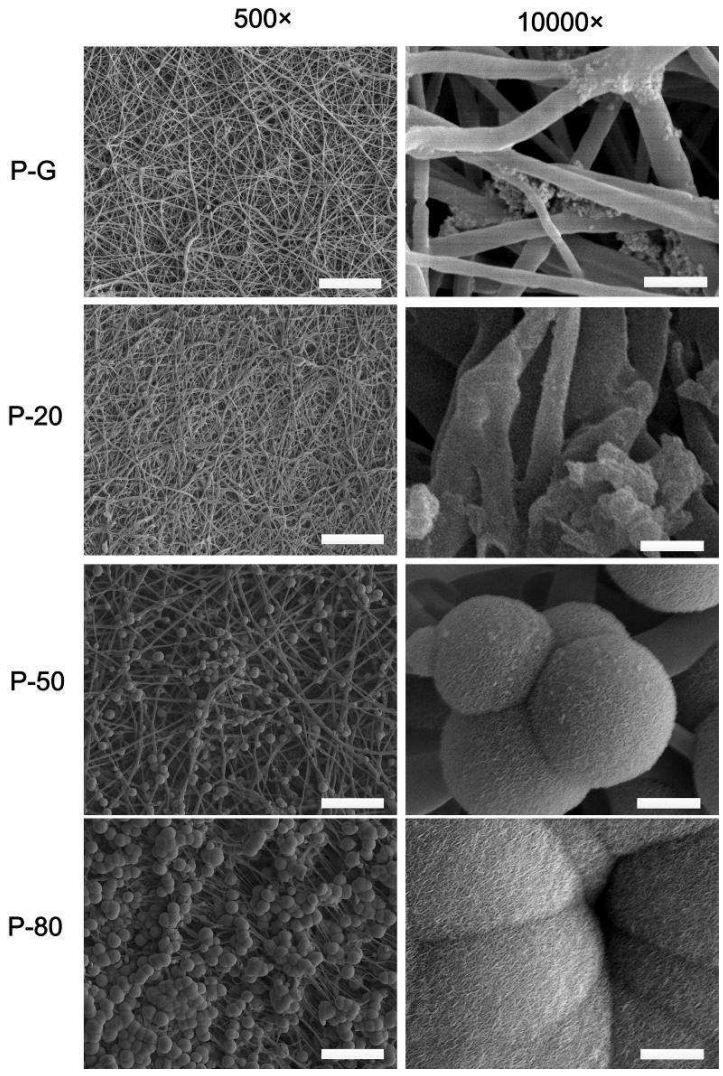

Fig. 4. Representative SEM images of composite fibrous membranes after soaking in SBF for 7 days. The left scale bar is 40 μm and the right scale bar is 2 μm.

In vitro biomineralization property of as-electrospun composite membranes were first evaluated by soaking in simulated body fluid (SBF) at 37°C for 21 days during which

SBF solution was not exchanged. Then samples were taken out for SEM, XRD and FITR analysis. As shown in Fig. S2, there was significant more crystal deposition on membrane with $CaCO_3$/casein than PCL and PCL with calcite. After mineralization, two additional diffraction peaks were observed on XRD pattern, where these two peaks were assigning to HAp (Fig. S3a); the absorption band of PO_4 was observed on FTIR spectra (Fig. S3b); EDS spectra also detected a large amount of P element (Fig. S3c). Based on these results, we can conclude that the presence of $CaCO_3$/casein vaterite particles enhanced the biomineralization of composite membrane.

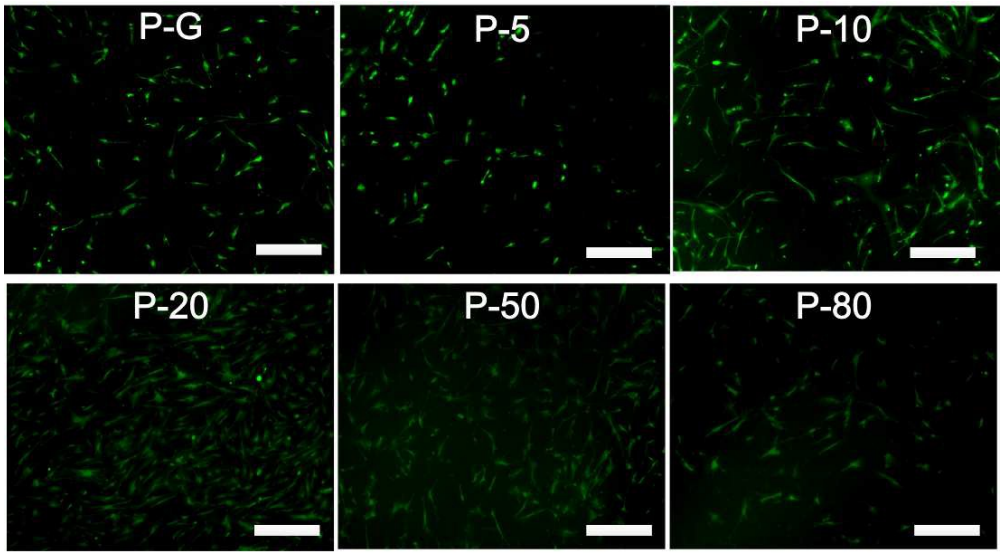

Fig. 5. Fluorescence microscope images of Human mesenchymal stem cells (HMSCs) on composite membranes after FDA staining on day 5. The scale bar is 200 μm.

For better mimicking ECM, modification of membrane surfaces were conducted. PCL is inert[6] (cells were round shaped on membranes without surface modification as shown in Fig. S4), so we modified the surface with cross-linking gelatin[10,22]. Representative samples P-G, P-20, P-50 and P-80 were selected for *in vitro* biomineralization evaluation. After immersion in SBF for 7 days, various amounts of crystals were deposited on different samples (Fig. 4). For P-G and P-20 membranes, only a few crystals were found in the pores of membrane in SEM images at larger magnification (Fig. 4, 2nd column). With the increase of $CaCO_3$/casein microspheres in membrane, a thin layer of crystals was observed on P-50 and P-80 surface. On P-50 surface, the crystal agglomerates were in spherical of size ~10 μm, while on P-80 surface, the agglomerates were much larger and their amount is much higher. Hence,

the enhancing effect on biomineralization was even improved after the surface modification and the biomineralization potential of composite membranes increased with $CaCO_3$/casein vaterite amount.

2.2 Cell Adhesion and proliferation test

Cell attachment and spreading on scaffolds is a crucial requirement for following cell activities. After FDA staining (Fig. 5) we can see on all membranes cells were spreading very well and in spindle shape. It seemed that more cells were on P-20 and P-50 membranes than others. Furthermore, cell proliferation was investigated using MTT assay. As shown in Fig. 6, the UV absorbance increased for all composite membranes from day 1 to 7, indicating the surface modification strategy was beneficial for cell proliferation. Among all samples, P-20 and P-50 membranes demonstrated higher absorbance values than the other membranes from day 3 to day 7, especially on day 7.

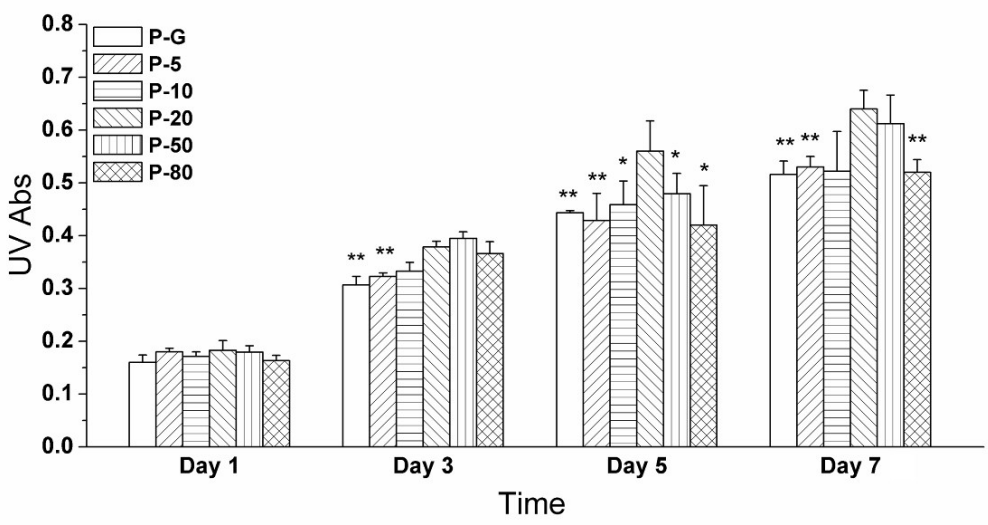

Fig. 6. MTT assay of HMSCs on composite membranes through 7 days' proliferation. (Data = mean ± standard deviation; n = 3; **p<0.01 versus P-20 group; *p<0.05 versus P-20 group; #p<0.05 versus P-50 group)

2.3 Cell differentiation investigation

$CaCO_3$ and casein have been proved to enhance calcification and differentiation of cells. The effects of composite membranes on differentiation of HMSCs were further investigated. The relative expression of osteogenic marker genes was analyzed by

RT-PCR. As shown in Fig. 7, the expression of ALP, COL-I, and RUNX-2 genes was the highest in HMSCs on P-20 membrane. Furthermore, the change of ALP activity of HMSCs on different membranes with differentiation time is shown in Fig. 8. From day 3 to 14, the ALP activity increased for all membranes, with the group P-20 demonstrating the peak value on days 7 and 14. When looking at ALP expression, it was interesting to find that the sample trend from the highest to the lowest gene expressions was nearly the same as that based on its activity on the same day. This consistence confirmed that our differentiation evaluation was well conducted. Thus, we can conclude that P-20 membrane showed the highest effect to enhance HMSCs osteogenic differentiation.

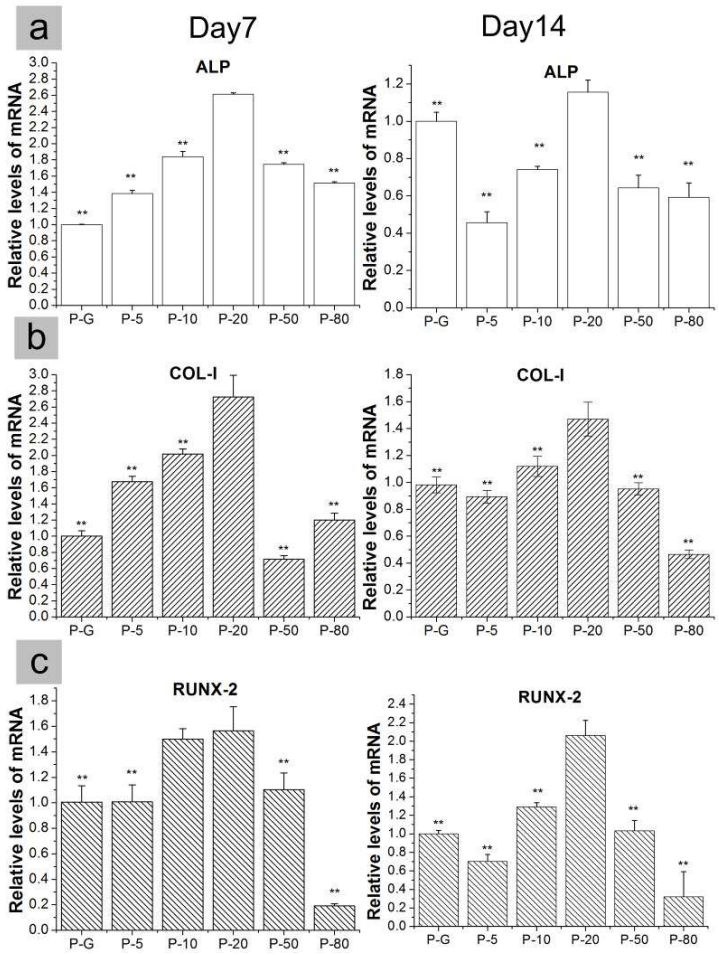

Fig. 7. Effects of different composite membranes on osteogenic gene expressions in HMSCs. (a) ALP, (b) COL-I, and (c) RUNX-2 gene expression on the P-20 composite fibrous membranes is significantly higher than that on the other membranes on days 7 and 14, except on day 7 cells on P-10 had close RUNX-2 gene expression as that on P-20. The relative gene

expression was normalized to the P-G group on the same day. (Data = mean ± standard deviation; n = 3; **p<0.01 versus P-20 group)

Both the proliferation and differentiation studies demonstrated that the enhancing effect did not increase with the concentration of $CaCO_3$/casein particles. It was probably because high amount of $CaCO_3$/casein would produce a rich Ca^{2+} microenvironment which exhibited negative effects on cells. Nevertheless, our results thus far showed that the composite membrane P-20 showed a potential towards developing an optimal osteoinductive and osteoconductive system.

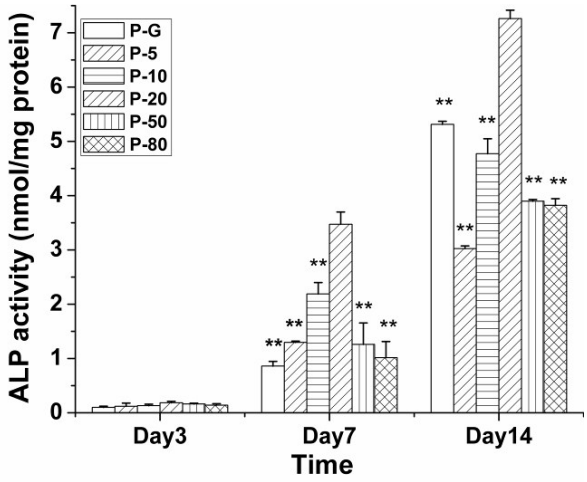

Fig. 8. ALP activity of HMSCs cultured on different composite fibrous membranes in osteogenic medium for various days. On days 7 and 14, ALP activity of cells on P-20 membrane was significantly higher than that on other membranes. (Data = mean ± standard deviation; n = 3; **p<0.01 versus P-20 group)

3. Conclusions

In this study, $CaCO_3$/casein hybrid microparticles were fabricated and further entrapped in PCL composite membranes to improve the *in vitro* biomineralization, cell proliferation and differentiation property. To find the optimum composition of membranes, $CaCO_3$/casein microspheres were entrapped at five different concentrations. The $CaCO_3$/casein microparticles were mainly in vaterite form based on XRD investigation. The presence of casein in microparticles was confirmed by FTIR analysis and BCA assay, where its content was determined to be 23.9 ± 1%. Casein affected the crystallization and stabilization of $CaCO_3$ in vaterite. All vaterite

microparticles were in spherical shape of 1 μm, where its size distribution was very narrow. Since PCL was hydrophobic and lacked functional groups for cell adhesion, surface modification of composite membranes was conducted. For sample P-50, the water contact angle decreased from 113.9 ± 3.7° to 66.4 ± 6.0°; the membrane morphology was not significantly changed with similar fiber diameter; both gelatin and casein were evenly distributed on the membrane. Due to the presence of vaterite microparticles, the biomineralization property of composite membrane was significantly enhanced, where the amount of HAp deposition increased with vaterite content. On composite membranes, HMSCs were spreading as spindles and proliferated very well, especially on sample P-20 and P-50. As for gene expressions of ALP, COL-I and RUNX-2 after cells induced to differentiation, the presence of $CaCO_3$/casein particles improved gene expressions, especially sample P-20 which had the highest level and also the highest ALP activity. Based on our studies, P-20 demonstrated better potential to be applied in bone tissue engineering and the *in vivo* performance will be conducted in future.

4. Experimental

4.1 Materials

Casein, dexamethasone, 3-(3-dimethylaminopropyl)-1-ethyl-carbodiimide hydrochloride (EDC), FDA, N-hydroxy-succinimide (NHS), rhodamine B, FITC, β-glycerophosphate, L-ascorbic acid, and PCL (Mw = 70000~90000) were purchased from Sigma-Aldrich (St, Louis, MO, USA). Sodium carbonate (Na_2CO_3), calcium chloride ($CaCl_2$), dichloromethane (DCM, 99.5%), dimethyl formamide (DMF, 99.5%), dimethylsulfoxide (DMSO, 99.0%), and ethanol were obtained from Guangzhou Chemical Reagent Co. (Guangzhou, Guangdong, China) and used without further purification. SBF was prepared following procedures as reported elsewhere[7] and all chemicals were from Sinopharm Chemical Reagent Co. Ltd (Shanghai, China). Alpha minimum essential medium (α-MEM) and PS (penicillin/streptomycin antibiotics) were purchased from HyClone (Logan, UT, USA). Fetal bovine serum (FBS) and trypsin-EDTA were purchased from GIBICO (Carlsbad, CA, USA). MTT and gelatin was from Amresco (Solon, OH, USA) and ALP assay kit was from Beyotime (Haimen, Jiangsu, China). Trizol reagent kit was from Invitrogen (CA,

USA), PrimeScript RT reagent kit was from TaKaRa (Mountain View, CA, USA), and GoTaq qPCR Master Mix was from Promega (Madison, WI, USA). Deionized (DI) ultrapure water was used throughout the experiment.

4.2 Preparation and characterization of the fibrous membranes

4.2.1 Fabrication of $CaCO_3$ particles in the presence of casein

The fabrication of $CaCO_3$/casein particles was performed as following. Casein (8 mg/ml) was dissolved in 50 mM Na_2CO_3 solution at room temperature. 50 mM $CaCl_2$ solution was rapidly poured into the casein-Na_2CO_3 solution at an equal volume under vigorous stirring (600 rpm). The mixture was stirred for 20 min. The precipitated $CaCO_3$/casein particles was centrifuged, washed with DI water three times, then dried through freeze-drying process and stored at room temperature before characterization.

The crystal phase and functional group characterization of the as-synthesized product was performed with XRD and FTIR spectroscopy. Surface morphology and particle size were investigated using a SEM (JEOL JSM-5600) with an accelerating voltage and a beam current at 15 kV and 10 mA, respectively. The casein content was measured with a BCA protein assay kit (Thermo Scientific Pierce, Rickford II, USA).

4.2.2 Preparation of the electrospun fibrous membrane

Two solvents, DCM and DMF were chosen as solvents for the electrospinning solution. These solvents have a very good miscibility. Fibrous membranes at various weight ratios of ($CaCO_3$/casein)/PCL as 0%, 5%, 10%, 20%, 50%, and 80% were fabricated. For this, electrospinning solutions were prepared as follows. $CaCO_3$/casein particles and PCL were suspended in DMF and dissolved in DCM respectively, and then mixed and stirred for 24 h at room temperature. The homogenous suspension was electrospun under a high voltage of 14 kV at a steady flow rate of 1.0 ml/h. The composite membranes were collected on an aluminum foil covered with coverslip glass which was 11 cm from the needle tip of the injector.

4.2.3 Immobilization of gelatin

The composite membranes were hydrolyzed in NaOH solution (1.5 M) at 4°C for 1 h to produce carboxyl groups, then washed extensively with DI water, and placed in HCl solution (10^{-6} M) for 3 min, followed by rinse with DI water three times again.

The membranes were further immersed in EDC/H_2O (8 mg/ml) and NHS/H_2O (2 mg/ml) solutions for 12 h at 4°C, followed by rinse with large amount of DI water. The membrane was then incubated in gelatin/PBS solution (2 mg/ml) for another 24 h at 4°C. As NaOH hydrolysis may have negative effects on casein in $CaCO_3$/casein particles, all membranes were incubated in casein (4 mg/ml in 25 mM Na_2CO_3) at 4°C for 12 h after gelatin grafting. Before seeding cells, membranes were immersed with gelatin (2 mg/ml) again for 15 min at 37°C. Various fibrous membranes P-G, P-5, P-10, P-20, P-50 and P-80 with weight ratios of ($CaCO_3$/casein)/PCL as 0%, 5%, 10%, 20%, 50%, and 80% were prepared (Scheme 1). The membrane morphology was observed with SEM. For the representative sample P-50, water contact angles were measured using a DSA100 system (Kruss, Hamburg, Germany).

To demonstrate the distribution of last adsorbed casein and gelatin on the membranes, the incubation process was performed using FITC labeled casein[15] and Rhodamine B labeled gelatin[27]. During the process, Olympus IX71 microscope (Olympus, Tokyo, Japan) was used to capture the fluorescent images and processed by Image-ProPlus software (Media Cybernetics, Rockville, MD, USA).

4.3 *In vitro* biomineralization assessment

Biomineralization properties of the membranes were evaluated by soaking in SBF at 37°C. The SBF was changed every 2 days, and after 7 days samples were removed from the medium, gently rinsed with DI water and dried at room temperature. The SEM images were taken to observe the surface morphology.

4.4 Cell adhesion assay

Before cell seeding, membranes were placed in 24-well tissue culture plates and sterilized by soaking in 75% alcohol and exposed to UV radiation for 30 min, then soaking in 10× PS for 12 h and washed 3 times with PBS. HMSC were seeded onto the composite membranes at a density of 8,000/ml and cultured with basal growth medium which was α-MEM containing 10% FBS at 37°C in 5% CO_2 humidified atmosphere for 7 days. The culture medium was changed every 2 days. On day 5, cells were washed with PBS and then incubated in FDA (5 μg/mL) solution at 37°C for 10 min. After rinse with PBS, fluorescent images were captured by Olympus IX71 microscope (Olympus, Tokyo, Japan).

During the 7 days of culture, MTT assay was used to investigate the cellular proliferation. Specifically, on days 1, 3, 5 and 7, 300 μl MTT (0.5 mg/ml) solution was added to each well and incubated at 37°C for 4 h in dark; 500 μl of DMSO was added to each well to dissolve the purple formazan crystal. Solution was transferred to a 96-well plate and the absorbance was measured at 570 nm using a microplate reader (BioTek Synergy4, USA).

4.5 *In vitro* osteoconductivity evaluation

4.5.1 Differentiation medium

For differentiation studies, HMSCs were seeded onto membranes in 24-well plates at a higher cell density (60,000 cells/ml) than that for proliferation studies. After cultured for 2 days in basal growth medium, HMSCs were induced to differentiation in osteogenic medium which was basal growth medium supplemented with 10 mM β-glycerophosphate, 0.2 mM L-ascorbic acid, and 0.1 μM dexamethasone for 14 days.

4.5.2 Analysis of gene expressions by real-time polymerase chain reaction (RT-PCR)

Total RNA was extracted from samples with Trizol reagent kit and was quantified with a microplate reader, followed by reverse transcription with the PrimeScript RT reagent kit.

Table 1. Primers sequences used for RT-PCR

Gene	Primer sequence (5'-3')	Gene Bank access number
GAPDH	F: AGAAAAACCTGCCAAATATGATGAC R: TGGGTGTCGCTGTTGAAGTC	NM_002046
COL-I	F: CAGCCGCTTCACCTACAGC R: TTTTGTATTCAATCACTGTCTTGCC	NM_000088.3
ALP	F: AGCACTCCCACTTCATCTGGAA R: GAGACCCAATAGGTAGTCCACATTG	NM_000478.3
RUNX2	F:AGAAGGCACAGACAGAAGCTTGA R:AGGAATGCGCCCTAAATCACT	NM_001015051.3

The quantification of gene expressions was carried out by RT-PCR using 20 ng of cDNA and GoTaq qPCR Master Mix following manufacturer's procedures. The primers were previously designed using the Primer 3 online software and synthesized by Invitrogen. The primer sequences of osteogenesis-related genes including COL-I, ALP, RUNX2 and the endogenous control gene GAPDH are listed in Table 1. Expression of these genes was analyzed from the cDNA (20 ng) and performed with ABI 7500 Real-time PCR Detector (Applied Biosystems, Foster City, CA, USA) and quantified via the $X=2^{-\Delta\Delta Ct}$ method, in which $\Delta\Delta C_t = \Delta E - \Delta C$, $\Delta E = C_{t\,exp} - C_{t\,GAPDH}$ and $\Delta C = C_{t\,ctrl} - C_{t\,GAPDH}$.

4.5.3 Measurement of ALP activity

The intracellular ALP activity was quantified using an ALP assay kit which was based on the conversion of corlorless *p*-nitrophenylphosphate (pNPP) to colored *p*-nitrophenol by ALP. The absorbance was measured at 405 nm using a microplate reaser. The amounts were normalized to the total intracellular protein content determined by the BCA protein assay kit and expressed in nanomoles of produced p-nitrophenol per mg of protein (nmol/mg).

4.6 Statistical analysis

Data are presented as mean ± standard deviation (SD) and were analyzed by one-way analysis of variance (ANOVA) test. $P < 0.05$ was consisdered to indicate a statistically significant difference.

Acknowledgements

This work was supported in part by the National Natural Science Foundation of China (51303216, 51103182 and 51203194), Guangdong Provincial Education Department (2013KJCX005), Science and Technology Planning Project of Guangdong Province (2011A060901013), and Guangdong Innovative Research Team Program (2009010057).

Notes and references

‡**Electronic Supplementary Information (ESI) available**: SEM images showed that

NaOH treatment resulted exposure of the entrapped $CaCO_3$/casein microparticles, while there was no significant change in fiber diameter; comparing $CaCO_3$/casein PCL composite membrane with PCL membrane and calcite PCL composite membrane, SEM showed that there was significantly more crystal deposition on PCL membrane with $CaCO_3$/casein, while XRD, FITR and EDS analysis confirmed that the deposited crystal was HAp; the cells morphology changed from round to spindle after surface modification.

1. B. A. Allo, S. G. Lin, K. Mequanint and A. S. Rizkalla, *Acs Applied Materials & Interfaces*, 2013, **5**, 7574-7583.
2. D. Bhuiyan, M. J. Jablonsky, I. Kolesov, J. Middleton, T. M. Wick and R. Tannenbaum, *Acta biomaterialia*, 2015, **15**, 181-190.
3. S. G. Caridade, C. Monge, J. Almodovar, R. Guillot, J. Lavaud, V. Josserand, J.-L. Coll, J. F. Mano and C. Picart, *Acta biomaterialia*, 2015, **15**, 139-149.
4. J. S. Carson and M. P. G. Bostrom, *Injury-International Journal of the Care of the Injured*, 2007, **38**, S33-S37.
5. K. D. Cashman, *British Journal of Nutrition*, 2002, **87**, S169-S177.
6. F. Chen, C. N. Lee and S. H. Teoh, *Mat Sci Eng C-Bio S*, 2007, **27**, 325-332.
7. A. Cuneyt Tas, *Journal of Non-Crystalline Solids*, 2014, **400**, 27-32.
8. C. G. de Kruif, T. Huppertz, V. S. Urban and A. V. Petukhov, *Advances in colloid and interface science*, 2012, **171-172**, 36-52.
9. A. O. Elzoghby, W. S. El-Fotoh and N. A. Elgindy, *Journal of controlled release : official journal of the Controlled Release Society*, 2011, **153**, 206-216.
10. M. Foox, A. Raz-Pasteur, I. Berdicevsky, N. Krivoy and M. Zilberman, *Polymers for Advanced Technologies*, 2014, **25**, 516-524.
11. M. S. Fourman, E. W. Borst, E. Bogner, S. R. Rozbruch and A. T. Fragomen, *Clinical Orthopaedics and Related Research*, 2014, **472**, 732-739.
12. M. Fujiwara, K. Shiokawa, K. Morigaki, Y. C. Zhu and Y. Nakahara, *Chemical Engineering Journal*, 2008, **137**, 14-22.
13. Y. P. Guo, Y. Zhou, D. C. Jia and H. X. Tang, *Microporous and Mesoporous Materials*, 2009, **118**, 480-488.
14. K. K. Gupta, A. Kundan, P. K. Mishra, P. Srivastava, S. Mohanty, N. K. Singh, A. Mishra and P. Maiti, *Physical Chemistry Chemical Physics*, 2012, **14**, 12844-12853.
15. J. Habibi, S. L. Brandt, T. A. Coudron, R. M. Wagner, M. K. Wright, E. A. Backus and J. E. Huesing, *Archives of Insect Biochemistry and Physiology*, 2002, **50**, 62-74.
16. M. I. Hassan, N. Sultana and S. Hamdan, *Journal of Nanomaterials*, 2014, DOI: 10.1155/2014/573238.
17. D. S. Horne, *Current Opinion in Colloid & Interface Science*, 2006, **11**, 148-153.
18. D. W. Hutmacher, *Biomaterials*, 2000, **21**, 2529-2543.
19. S. Kim and C. B. Park, *Advanced Functional Materials*, 2013, **23**, 10-25.

20. Y. Koo, H. Lee, S. Kim, N. J. Song, J. M. Ku, J. Lee, C. H. Choi, K. W. Park and G. Kim, *Rsc Adv*, 2015, **5**, 44943-44952.
21. A. López-Marzo, J. Pons and A. Merkoçi, *Journal of Materials Chemistry*, 2012, **22**, 15326.
22. H. Layman, M. G. Spiga, T. Brooks, S. Pham, K. A. Webster and F. M. Andreopoulos, *Biomaterials*, 2007, **28**, 2646-2654.
23. S. S. Lee, B. J. Huang, S. R. Kaltz, S. Sur, C. J. Newcomb, S. R. Stock, R. N. Shah and S. I. Stupp, *Biomaterials*, 2013, **34**, 452-459.
24. P. Liang, D. Zhao, C.-Q. Wang, J.-Y. Zong, R.-X. Zhuo and S.-X. Cheng, *Colloids and Surfaces B: Biointerfaces*, 2013, **102**, 783-788.
25. C.-H. Lin, S.-h. Hsu, J.-M. Su and C.-W. Chen, *Journal of Tissue Engineering and Regenerative Medicine*, 2011, **5**, 156-162.
26. A. Martins, A. R. C. Duarte, S. Faria, A. P. Marques, R. L. Reis and N. M. Neves, *Biomaterials*, 2010, **31**, 5875-5885.
27. K. Morimoto, S. Chono, T. Kosai, T. Seki and Y. Tabata, *Journal of Pharmacy and Pharmacology*, 2005, **57**, 839-844.
28. P. M. Mountziaris, S. N. Tzouanas and A. G. Mikos, *Biomaterials*, 2010, **31**, 1666-1675.
29. G. Pitarresi, C. Fiorica, F. S. Palumbo, F. Calascibetta and G. Giammona, *Journal of Biomedical Materials Research Part A*, 2012, **100A**, 1565-1572.
30. J. Pu, F. Yuan, S. Li and K. Komvopoulos, *Acta Biomaterialia*, 2015, **13**, 131-141.
31. I. Rajzer, E. Menaszek, R. Kwiatkowski, J. A. Planell and O. Castano, *Materials Science & Engineering C-Materials for Biological Applications*, 2014, **44**, 183-190.
32. M. G. Raucci, V. D'Anto, V. Guarino, E. Sardella, S. Zeppetelli, P. Favia and L. Ambrosio, *Acta Biomaterialia*, 2010, **6**, 4090-4099.
33. C. Ru, F. Wang, M. Pang, L. Sun, R. Chen and Y. Sun, *Acs Applied Materials & Interfaces*, 2015, **7**, 10872-10877.
34. S. Stocks-Fischer, J. K. Galinat and S. S. Bang, *Soil Biology & Biochemistry*, 1999, **31**, 1563-1571.
35. W. L. Suchanek, P. Shuk, K. Byrappa, R. E. Riman, K. S. TenHuisen and V. F. Janas, *Biomaterials*, 2002, **23**, 699-710.
36. S. Tugulu, R. Barbey, M. Harms, M. Fricke, D. Volkmer, A. Rossi and H. A. Klok, *Macromolecules*, 2007, **40**, 168-177.
37. S. G. Vallejo-Heligon, B. Klitzman and W. M. Reichert, *Acta Biomaterialia*, 2014, **10**, 4629-4638.
38. D. V. Volodkin, S. Schmidt, P. Fernandes, N. I. Larionova, G. B. Sukhorukov, C. Duschl, H. Mohwald and R. von Klitzing, *Advanced Functional Materials*, 2012, **22**, 1914-1922.
39. C. Y. Wan and B. Q. Chen, *Biomedical Materials*, 2011, **6**.
40. Y. Wang, Y. X. Moo, C. Chen, P. Gunawan and R. Xu, *Journal of colloid and interface science*, 2010, **352**, 393-400.
41. A. M. Wojtowicz, A. Shekaran, M. E. Oest, K. M. Dupont, K. L. Templeman, D. W. Hutmacher, R. E. Guldberg and A. J. Garcia, *Biomaterials*, 2010, **31**, 2574-2582.
42. G. Xu, X. Wang, C. Deng, X. Teng, E. J. Suuronen, Z. Shen and Z. Zhong, *Acta biomaterialia*, 2015, **15**, 55-64.
43. Z. Xu, G. Liang, L. Jin, Z. Wang, C. Xing, Q. Jiang and Z. Zhang, *Journal of Crystal Growth*, 2014, **395**, 116-122.
44. M. Yamamoto, Y. Takahashi and Y. Tabata, *Tissue Engineering*, 2006, **12**, 1305-1311.
45. A. M. Yousefi, M. E. Hoque, R. Prasad and N. Uth, *Journal of Biomedical Materials Research Part A*,

2015, **103**, 2460-2481.

46. A. Zajicova, E. Javorkova, P. Trosan, M. Krulova and V. Holan, *Journal of Tissue Engineering and Regenerative Medicine*, 2014, **8**, 277-278.
47. X. Zhang, V. Thomas and Y. K. Vohra, *Journal of Materials Science-Materials in Medicine*, 2010, **21**, 541-549.

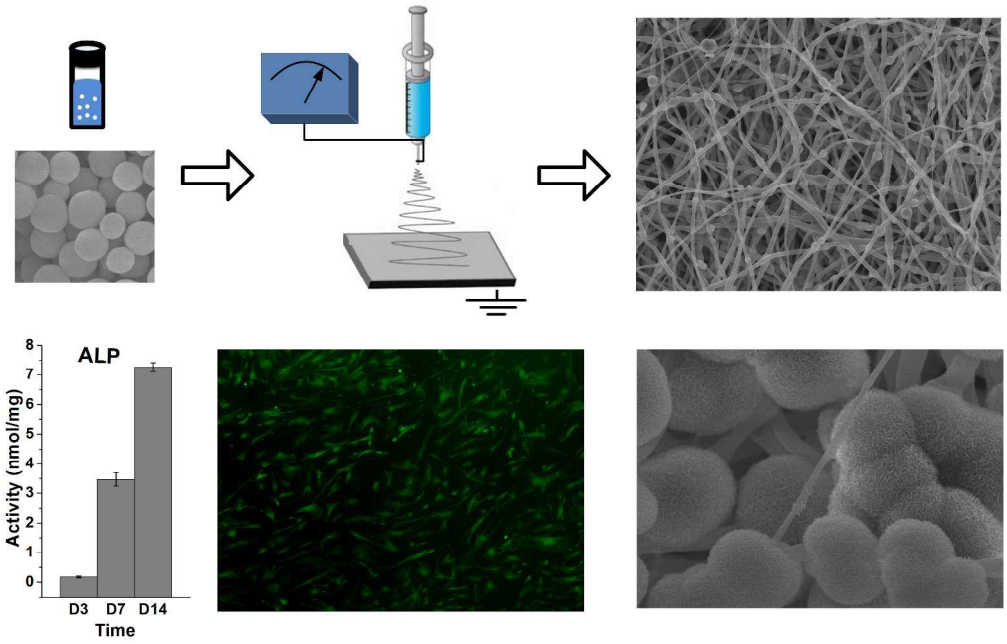

286x184mm (300 x 300 DPI)